Check for
updates

Algal-Mediated Priming Effects on the Ecological Stoichiometry of Leaf Litter Decomposition: A Meta-Analysis

Halvor M. Halvorson[1], Steven N. Francoeur[2], Robert H. Findlay[3] and Kevin A. Kuehn[1]*

[1] University of Southern Mississippi School of Biological, Environmental, and Earth Sciences, Hattiesburg, MS, United States,
[2] Eastern Michigan University Department of Biology, Ypsilanti, MI, United States, [3] Department of Biological Sciences, The University of Alabama, Tuscaloosa, AL, United States

In aquatic settings, periphytic algae exude labile carbon (C) that can significantly suppress or stimulate heterotrophic decomposition of recalcitrant C via priming effects. The magnitude and direction of priming effects may depend on the availability and stoichiometry of nutrients like nitrogen (N) and phosphorus (P), which can constrain algal and heterotrophic activity; in turn, priming may affect heterotrophic acquisition not only of recalcitrant C, but also N and P. In this study, we conducted a meta-analysis of algal-mediated priming across leaf litter decomposition experiments to investigate (1) bottom-up controls on priming intensity by dissolved N and P concentrations, and (2) effects of algal-mediated priming on the fate of litter-periphyton N and P during decomposition. Across a total of nine datasets, we quantified priming intensity and tested algal effects on litter-periphyton C:N, C:P, and N- and P-specific mass loss rates. Algal effect sizes did not significantly differ from zero, indicating weak or inconsistent algal effects on litter-periphyton stoichiometry and nutrient loss. These findings were likely due to wide variation in algal priming intensity across a limited number of experiments, ranging from strongly negative (410% reduced decomposition) to strongly positive (104% increased decomposition). Correlation and response surface analyses showed that priming intensity switched from negative to positive with increasing dissolved inorganic N:P across datasets. Algal effects on litter-periphyton stoichiometry and nutrient loss further co-varied with dissolved N:P across datasets, suggesting algae most strongly influence the stoichiometry of decomposition under imbalanced N:P, when priming is most intense. Our findings from this limited meta-analysis support the need for additional tests of aquatic priming effects, especially across gradients of N and P availability, with consideration of coupled C and nutrient dynamics during priming of organic matter decomposition.

Keywords: carbon, nitrogen, phosphorus, mineralization, immobilization, priming effects, detritus, streams

INTRODUCTION

Decomposition of organic matter, such as plant litter, represents a major flux of carbon (C) and nutrients in many ecosystems because the majority of plant biomass ultimately enters the detrital pool (Cebrian, 1999; Moore et al., 2004). Heterotrophic microbes, including fungi and bacteria, colonize organic matter and synthesize degradative enzymes to acquire organic C, nitrogen (N), and phosphorus (P) from plant litter, thus driving decomposition over time (Romaní et al., 2006; Sinsabaugh and Follstad Shah, 2012; Sinsabaugh et al., 2014). Additions of exogenous organic C and inorganic N and P can alter this decomposition process by supplementing heterotrophic investment in degradative enzymes and directly stimulating heterotrophic growth rates, which in turn may enhance rates of decomposition (Carreiro et al., 2000; Kuehn et al., 2014; Jabiol et al., 2018). In particular, recent research has revealed an important role of labile organic C additions, such as plant exudates or glucose, in stimulating microbial degradation of comparatively recalcitrant organic C by as much as 382% (Kuzyakov, 2010; Danger et al., 2013; Cheng et al., 2014). However, recent research in aquatic systems indicates that the presence of algal exudates (considered a source of labile C) can elicit wide-ranging effects, from significant enhancement (Danger et al., 2013) to significant inhibition (Halvorson et al., 2019), of leaf litter decomposition rates. As a consequence, the "priming effect" phenomenon appears to elicit a wide potential to alter the fate of organic C and nutrients across many ecosystems (Guenet et al., 2010, 2018), yet the interplay between priming and nutrient dynamics during organic matter decomposition remains poorly studied (Chen et al., 2014; Li et al., 2018).

Ecological stoichiometry theory (Sterner and Elser, 2002) provides a framework to relate priming effects to nutrient availability and nutrient mineralization/immobilization during microbial decomposition of organic matter. In particular, stoichiometry may be used to investigate (1) responses of microbial decomposer growth and activity to the supply of N and P (Mooshammer et al., 2012; Manning et al., 2015) and (2) coupling of N and P mineralization and immobilization relative to mineralization of C during organic matter decomposition (Manzoni et al., 2010). While priming effects are concerned primarily with interactions between labile and recalcitrant C pools, priming intensity (defined as priming direction and magnitude) may be controlled by stoichiometric constraints, because heterotrophic acquisition of N and P is also necessary to trigger increased heterotrophic activity and enzyme production in response to labile C additions (Chen et al., 2014). For example, the "microbial N-mining" hypothesis proposes that priming intensity may increase with N-limitation, because heterotrophs use labile C additions to invest in degradative enzymes to acquire limiting organic-bound N, thereby enhancing organic matter decomposition (Moorhead and Sinsabaugh, 2006; Chen et al., 2014; Soares et al., 2017). Recent evidence from terrestrial soils supports this hypothesis, including reduced priming intensities in N-rich soils. Such data imply that the priming effect phenomenon may alleviate terrestrial plant nutrient limitation by increasing

the recycling of organic nutrients within soils (Meier et al., 2017; Fang et al., 2018).

The ecological stoichiometry of priming effects remains comparatively understudied in aquatic systems, where priming can be significant (e.g., Danger et al., 2013; Bianchi et al., 2015), yet the general direction and magnitude of priming effects are strongly debated due to incongruent evidence (Bengtsson et al., 2018; Elosegi et al., 2018). Some studies suggest that increased dissolved N and P concentrations may shift priming from positive to negative, by stimulating algal growth and exudation of labile C and enabling preferential use of labile C by microbial heterotrophs in lieu of recalcitrant detrital C (Guenet et al., 2010; Guillemette et al., 2016). These trends in priming intensity are supported across two leaf litter decomposition studies showing a shift from positive to neutral or negative algal-mediated priming with increased nutrient concentrations (Danger et al., 2013; Halvorson et al., 2016). However, studies of dissolved organic matter have found weak relationships between priming and nutrient availability (Hotchkiss et al., 2014; Catalán et al., 2015), possibly because coupling between priming and nutrient availability is more diffuse within the water column compared to spatially-constrained interactions within biofilms colonizing organic matter (Bengtsson et al., 2018). Algae are present even in well-shaded aquatic ecosystems (Greenwood and Rosemond, 2005; Elosegi et al., 2018) and form mixed heterotrophic and autotrophic biofilms (e.g., periphyton) on organic substrata, which may be hotspots of priming and nutrient mineralization/immobilization (Kuehn et al., 2014; Battin et al., 2016; Wagner et al., 2017). For example, algal exudation of labile C may stimulate fungal N mineralization from underlying organic matter (Soares et al., 2017). Thus, the algal-heterotrophic consortium in periphyton represents an ideal experimental system to investigate the stoichiometry of priming effects including (1) bottom-up controls of dissolved N and P concentrations on the direction and strength of algal-heterotroph interactions underlying priming (Scott et al., 2008; Demars et al., 2018), and (2) implications of priming for heterotrophic acquisition and mineralization of N and P from recalcitrant organic matter (Guenet et al., 2010).

In the present study, we investigated the interplay of nutrient stoichiometry (available dissolved N and P, and litter-periphyton coupled C, N and P dynamics) with algal-mediated priming effects on leaf litter decomposition in aquatic ecosystems. We used a meta-analysis of prior experiments to test algal effects on leaf litter-periphyton C:N and C:P, as well as N- and P-specific mass loss rates, as indicators of priming effects on leaf decomposition beyond direct priming of C mineralization, which has been the focus of prior synthesis (e.g., Bengtsson et al., 2018). We hypothesized that across studies (1) priming intensity, and therefore algal-mediated changes in litter stoichiometry, would be weaker under increased dissolved nutrient availability (Guenet et al., 2010), (2) algae would decrease litter-periphyton C:N and C:P by enhancing the mineralization of litter C and supplementing periphyton with N- and P-rich biomass, and (3) by comparison, algae would elicit weak effects on N- and P-specific mass loss, because algal immobilization would counterbalance increased

heterotrophic mineralization of organic N and P due to priming (Halvorson et al., 2016).

MATERIALS AND METHODS

Literature Survey for Meta-Analysis

We conducted a meta-analysis to investigate how algae affect leaf litter stoichiometry during decomposition. On August 3, 2018 we surveyed the literature for relevant studies using Web of Science, employing the topic search terms [(ALGA* OR "LIGHT") AND DECOMPOS* AND ("STREAM" OR "AQUATIC" OR "LAKE" OR "WETLAND") AND ("PHOSPHORUS" OR "NITROGEN" OR STOICH*)]. We assessed all 260 resultant publications for potential use in the meta-analysis. To meet criteria for inclusion in the meta-analysis, studies needed to compare leaf litter decomposition in the presence versus absence of algae, such as by experimental shading. Studies also needed to report both mass loss and litter-periphyton elemental contents (e.g., molar C:N, C:P) during decomposition. A total of three published studies met criteria for inclusion, which we supplemented with two then-unpublished experimental datasets of our own (**Table 1**). For a description of methods used to collect unpublished data, see **Supplementary Material Appendix 1**. Some of the studies in our meta-analysis included experiments using different nutrient levels (Danger et al., 2013; Halvorson et al., 2016) or contrasting leaf species (Halvorson et al., 2019) and we considered each dataset from these contrasting conditions as a separate contribution to calculate an algal effect size. Although there is a common first-author among many of these datasets (present first-author), indicating possible non-independence of the data, each of these datasets was collected by a different group of scientists in a different experimental setting. For the 2016 and 2019 published datasets, the first-author analyzed the data and led manuscript generation, but the second-author of each study (both students) was primarily responsible for data generation.

Effect Size Calculations

From each dataset, we identified the leaf litter species used, concentrations of available dissolved inorganic N (DIN; $N-NO_3 + N-NH_4$) and dissolved inorganic P (DIP; $P-PO_4$), sample sizes, and initial leaf litter molar C:N:P contents (**Table 1** and **Supplementary Table S1**). We also extracted data regarding dry mass loss, litter-periphyton molar C:N and C:P, and proportion initial N and P remaining during decomposition. We calculated exponential dry mass loss rate coefficients k (d^{-1}) based on the negative log-transformed slope of litter-periphyton dry mass remaining over time (Bärlocher, 2005). We subsequently calculated algal priming intensity as an indicator of algal-mediated priming effects using the log response ratio (lnRR) in equation 1

$$priming\ intensity = ln\frac{k_{algae\ present}}{k_{algae\ absent}} \quad (1)$$

Positive values of priming intensity thus indicate algae stimulated litter decomposition, whereas negative values indicate algae inhibited litter decomposition.

TABLE 1 | Summary of nine datasets used in the meta-analysis of the stoichiometry of algal-mediated priming effects during leaf litter decomposition.

Citation[a]	Leaf species	Sample size (n)	Priming intensity[b]	DIN (ug/L)	DIP (ug/L)	Molar N:P
1	Acer saccharum	3	0.71	1527	10.6	318.6
1	Acer saccharum	3	−0.22	1527	60.6	55.7
1	Acer saccharum	3	−1.45	1527	511	6.61
2	Liriodendron tulipifera[c]	4	−0.86	40.8	366	0.25
2	Quercus nigra[c]	4	−1.63	40.8	366	0.25
3	Alnus glutinosa	4	0.43	560	60	20.6
3	Alnus glutinosa	4	−0.01	5600	600	20.6
4	Zea mays	3	−0.08	600	200	6.63
5	Typha domingensis[c]	6	−1.59	15.6	15	2.30

*Datasets are identified by leaf species used, sample size in each treatment, observed priming intensity, dissolved inorganic nitrogen (DIN), and dissolved inorganic phosphorus (DIP), and dissolved molar N:P. See **Supplementary Table S1** for initial leaf litter molar C:N:P contents. [a]Citations: [1]Halvorson et al. (2016), [2]Halvorson et al. (2019), [3]Danger et al. (2013), [4]Soares et al. (2017), [5]Halvorson et al. (unpublished). [b]Calculated using Equation 1. [c]Datasets used for calculation of microbial and litter pools of C, N, and P at the end of decomposition (**Figure 5**).*

From each study, we used dry mass loss over time to identify three discrete stages of decomposition, to examine if algal effect sizes vary with stage of decomposition. Because mass loss rates and study duration varied widely across datasets, we identified mass loss stages based on mass loss around general guidelines of early (∼ <25% mass loss), mid (∼25–50% mass loss), and late (∼ >50% mass loss). These stages equated to mass loss of mean ± SE 15.4 ± 5.2% (early), 28.1 ± 5.1% (mid), and 44.0 ± 4.8% (late) in the fastest-decomposing treatments within each dataset. Across all time points within each stage, we calculated average litter-periphyton C:N and C:P in algae-present and algae-absent treatments. We then calculated an algal effect size on C:N and C:P based on lnRR calculated at each stage using equation 2

$$Algal\ nutrient\ ratio\ effect\ size = ln\frac{C:X_{algae\ present\ i}}{C:X_{algae\ absent\ i}} \quad (2)$$

where X = either N or P and i = early, mid, or late stages of decomposition. In this way, positive effect sizes indicate algae increase litter-periphyton C:N or C:P and negative effect sizes indicate algae decrease litter-periphyton C:N or C:P.

We also assessed how algae affected litter-periphyton stoichiometry during overall decomposition by calculating average C:N and C:P throughout the duration of each dataset in algae-present and algae-absent treatments. Similar to above, we then calculated algal effect sizes on litter-periphyton C:N and C:P using lnRR, with mean ratio of the algae-present treatment in the numerator and the algae-absent treatment in the denominator.

Studies also provided sufficient data to calculate litter-periphyton N- and P-specific mass loss rates k_N and k_P, respectively. We calculated these loss rates based on the negative

log-transformed slope of proportion of initial N and P remaining over time. In some datasets, litter exhibited net increases in total N and P (net immobilization), indicated by negative k_N and k_P values. Because some values were negative, lnRR could not be calculated. Instead, we used Hedge's d as the algal effect size on k_N and k_P by subtracting the mean k_N or k_P in algae-absent treatments from mean k_N or k_P in the algae-present treatments and dividing by the pooled standard deviation corrected for small sample size bias (Hedges and Olkin, 1985). Positive effect sizes thus indicate algae increase litter-periphyton N- or P-specific mass loss rates.

Statistical Analysis and Response Surfaces

We estimated variance associated with effect sizes from each dataset using sample sizes and standard deviation of each treatment mean following Rosenberg et al. (2013). All effect sizes and variances may be found in **Supplementary Material Appendix 2**. We used weighted mixed effects models (weight = 1/variance) to test differences in effect sizes across stages of decomposition (C:N and C:P) using decomposition stage as a fixed effect and dataset identity as a random effect (Rosenberg, 2013). In this way, the model accounts for heterogeneity (e.g., differing nutrient availability or leaf litter species) across studies. For all other effect sizes (C:N or C:P during overall decomposition, k_N or k_P) we used one-sample weighted t-tests (weight = 1/variance) to test whether effect sizes differed from a null hypothesis of zero, indicating no algal effect on a given response variable, using the R package "weights" (Pasek, 2018). For each analysis, we calculated heterogeneity of effect sizes using the statistic I^2, which describes proportional heterogeneity attributable to random between- relative to within-study variance (Senior et al., 2016). See the **Supplementary Material Appendix 3** for our R code to conduct the mixed effects models and determine I^2. We also calculated statistical power of all t-tests used to compare effect sizes to a null hypothesis of zero using the R package "pwr" (Champely, 2018). Finally, as a diagnostic of small-study effects or publication bias, we created funnel plots for each of the four effect sizes analyzed using t-tests (Sterne and Harbord, 2004; Jennions et al., 2013; see **Supplementary Figure S1**). We report summary statistics of models and analyses in **Table 2**. All statistical analyses were performed using R version 3.5.1 (R Core Team, 2018).

We employed the R package "fields" (Nychka et al., 2018) to create thin-plate splines (fitted lambda = 0.1) and response surfaces (Sperfeld et al., 2016) to visualize patterns in priming intensity and algal effect sizes across the gradient of DIN and DIP associated with all datasets (**Table 1**). These visualizations illustrate how variable dissolved N and P concentrations affect the magnitude and direction of priming intensity as well as algal effect sizes on litter-periphyton stoichiometry during decomposition. As a *post-hoc* analysis of trends revealed in the response surfaces, we calculated Pearson's correlation coefficients r to examine relationships between $\log_{10}$ dissolved molar DIN:DIP and each of algal priming

TABLE 2 | Summary of meta-analysis response variables, metrics of effect size, number of datasets included, heterogeneity statistics I^2, random effects variance, and statistical power of mixed effects models.

Response variable	Effect size	# Datasets	I^2	Random effects variance	Statistical power[a]
Stage-specific C:N	lnRR	27	78.2%	0.008	
Stage-specific C:P	lnRR	24	92.0%	0.089	
Overall C:N	lnRR	9	79.8%	0.011	0.32
Overall C:P	lnRR	8	57.5%	0.005	0.05
k_N	Hedge's d	9	45.2%	0.497	0.34
k_P	Hedge's d	8	69.7%	1.537	0.41

See **Supplementary Material Appendix 2** for effect sizes and variance associated with each dataset. [a]Power to test a null hypothesis that effect size differed from a mean of zero (one-sample two-tailed t-test; P < 0.05).

intensity, algal effect sizes on C:N and C:P, and algal effect sizes on k_N and k_P.

Budgeting Algal Effects on C, N, and P Pools During Decomposition

A subset of three datasets from *Liriodendron tulipifera*, *Typha domingensis*, and *Quercus nigra* decomposition quantified litter-periphyton C as well as C-specific biomass of major microbial pools (algae, fungi, bacteria), and were suitable for an exercise quantifying major pools of C, N, and P at the end of decomposition in the presence versus absence of algae (**Table 1**). Our calculations relied upon some assumptions about the stoichiometry of each microbial group; we assumed that algae exhibit molar C:N and C:P of 23 and 358, respectively, representative of N-limited algae given all included datasets were drawn from dissolved molar N:P < 4 (Kahlert, 1998). We assumed fungi exhibit molar C:N and C:P of 11 and 107, respectively; fungi appear to be strictly homeostatic in C:N but may have exhibited lower C:P under high-P conditions, causing potentially underestimated fungal P contents (Gulis et al., 2017). Finally, we assumed bacteria exhibit molar C:N and C:P of 4.3 and 28, respectively, assuming conditions were P-sufficient for bacteria within the periphyton complex (Godwin and Cotner, 2015).

In each of the three datasets included, we calculated C, N, and P associated with algal, bacterial, and fungal biomass and subtracted from total litter-periphyton pools (dry mass multiplied by litter-periphyton %C, %N, or %P) measured on the final day of decomposition. We attributed remaining (unaccounted) elemental pools to detritus, which includes both residual litter and accumulated microbial necromass. We then calculated how final pools of C, N, and P compared proportionally to endogenous litter C, N, and P (e.g., per unit dry mass) at the beginning of decomposition. In this way, we calculated how total pools of each element at the end of decomposition compared proportionally to initial available pools within the litter. Because microbes can assimilate exogenous N and P, these nutrient proportions often exceeded 1.0.

RESULTS

Priming Intensity Across Studies

The literature survey revealed substantial variation in the magnitude and direction of algal-mediated priming effects across leaf decomposition studies (**Table 1**). Priming intensity ranged from strongly negative (priming intensity = −1.63; 410% decreased mass loss with algae present) to strongly positive (priming intensity = 0.71; 104% increased mass loss with algae present). Plotted as a response surface across the gradient of DIN and DIP, priming intensities tended to be negative under low dissolved N:P and positive under high dissolved N:P conditions, exhibiting an apparent switchpoint between molar N:P of 16 and 64 (**Figure 1**). Algal priming intensity was strongly positively correlated to dissolved molar N:P across datasets ($r = 0.772$, $P = 0.015$; **Supplementary Figure S2A**), while priming intensity was not significantly correlated with either DIN or DIP concentrations ($r = 0.648$, $P = 0.059$ and $r = -0.327$, $P = 0.391$, respectively).

Algal Effects on Leaf Litter Stoichiometry During Decomposition

Algal effect sizes on leaf litter C:N did not differ across the three major stages of decomposition ($F_{2,24} = 1.6$, $P = 0.224$) but did exhibit a trend of shifting from positive during early and mid-decomposition to negative during late-decomposition (**Figure 2A**), indicating algae tend to increase litter C:N early and decrease litter C:N during later stages of decomposition. Collectively, algae did not significantly affect litter-periphyton C:N during overall decomposition ($t_{1,8} = 0.84$; $P = 0.428$; **Figure 2B**).

Similarly, algal effect sizes on standing litter C:P did not differ across the differing stages of decomposition ($F_{2,21} = 0.4$; $P = 0.688$), but algal effects on C:P followed a similar pattern as algal C:N effect sizes, shifting from positive to negative during late stages of decomposition (**Figure 2C**). In addition, algal effects on litter-periphyton C:P during overall decomposition did not differ from zero ($t_{1,7} = 0.04$; $P = 0.967$; **Figure 2D**).

Algal effects on litter-periphyton N- and P-specific mass loss rates did not differ from zero ($t_{1,8} = -0.59$, $P = 0.571$ and $t_{1,7} = -0.59$, $P = 0.576$, respectively). Effect sizes were on average negative, indicating algae tend to slow N- and P-specific mass loss during decomposition (**Figure 3**), likely through increased microbial immobilization.

Algal Effect Sizes Across Gradients of Dissolved N and P

The response surfaces indicated that, similar to trends in priming intensity, DIN and DIP concentrations may drive trends in algal effect sizes on litter-periphyton stoichiometry during decomposition (**Figure 4** and **Supplementary Figure S2**). Algal effect sizes on litter-periphyton C:N and C:P shifted from positive under low-N:P conditions, to negative under high-N:P conditions (**Figures 4A,C**), indicating algae either diluted or enriched litter-periphyton N and P relative to C pools, depending on dissolved nutrient stoichiometry. Algal effect sizes on C:N
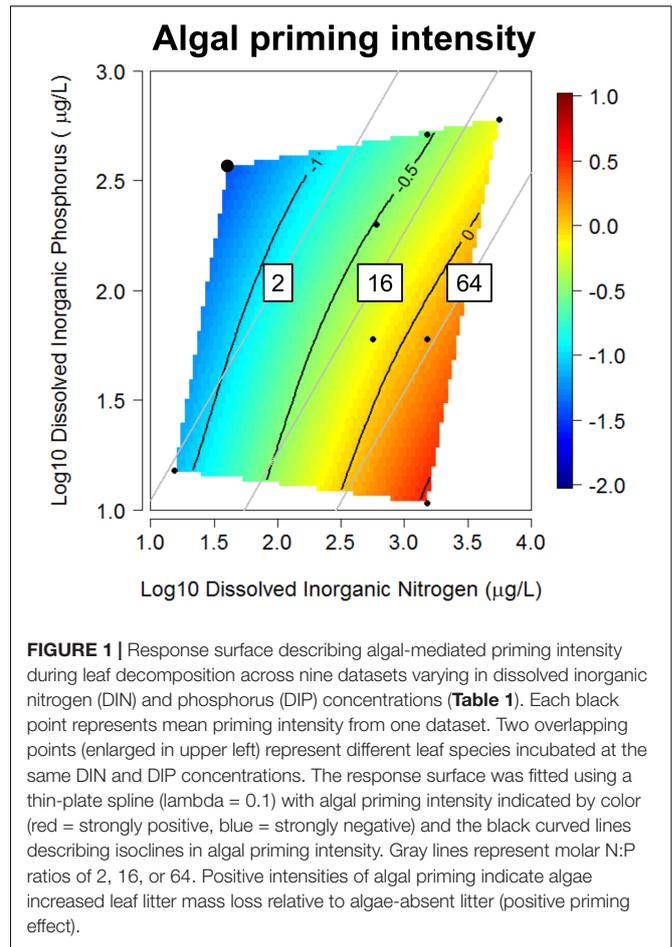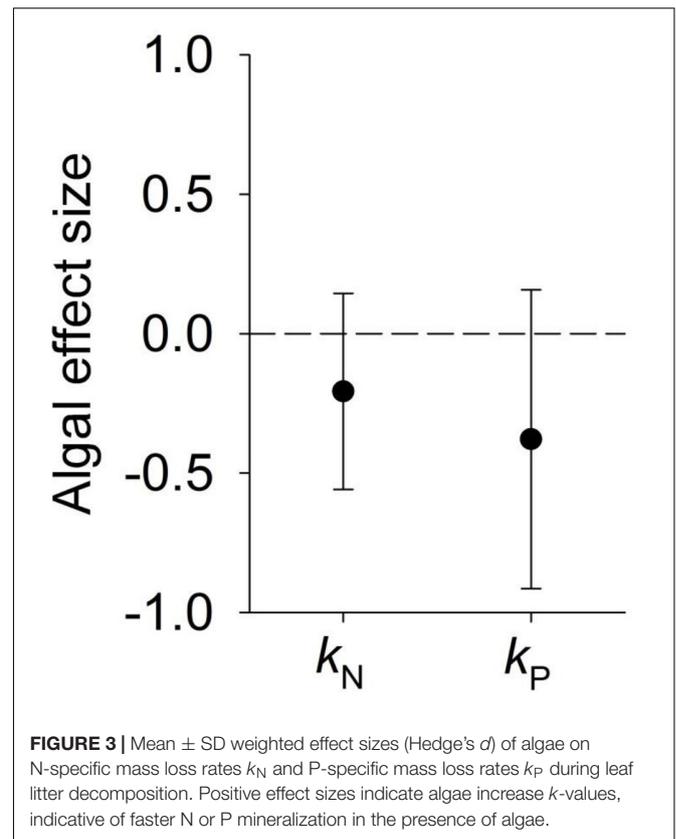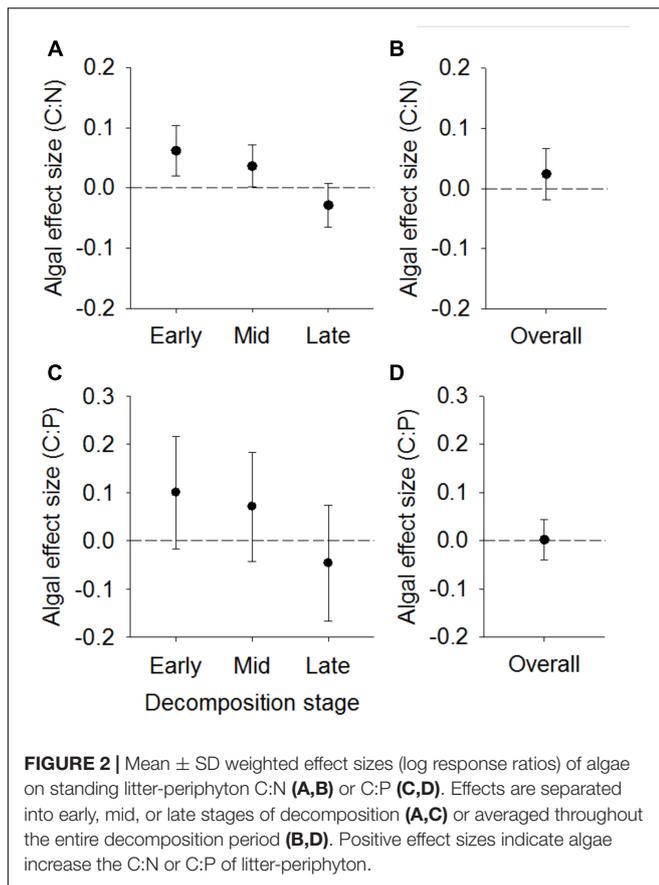

FIGURE 1 | Response surface describing algal-mediated priming intensity during leaf decomposition across nine datasets varying in dissolved inorganic nitrogen (DIN) and phosphorus (DIP) concentrations (**Table 1**). Each black point represents mean priming intensity from one dataset. Two overlapping points (enlarged in upper left) represent different leaf species incubated at the same DIN and DIP concentrations. The response surface was fitted using a thin-plate spline (lambda = 0.1) with algal priming intensity indicated by color (red = strongly positive, blue = strongly negative) and the black curved lines describing isoclines in algal priming intensity. Gray lines represent molar N:P ratios of 2, 16, or 64. Positive intensities of algal priming indicate algae increased leaf litter mass loss relative to algae-absent litter (positive priming effect).

were strongly negatively correlated with dissolved molar N:P ($r = -0.674$, $P = 0.047$; **Supplementary Figure S2B**) whereas algal effect sizes on C:P were weakly negatively correlated with dissolved molar N:P ($r = -0.592$, $P = 0.122$; **Supplementary Figure S2C**). In turn, algae tended to increase N- and P-specific mass loss under high-N:P scenarios, but decrease N- and P-specific mass loss under low-N:P scenarios (**Figures 4B,D**). Algal effect sizes on k_N were strongly positively correlated with dissolved molar N:P ($r = 0.690$, $P = 0.040$; **Supplementary Figure S2D**) and algal effect sizes on k_P were weakly positively correlated with dissolved molar N:P ($r = 0.649$, $P = 0.081$; **Supplementary Figure S2E**).

Budgeting Algal Effects on C, N, and P Pools During Litter Decomposition

Comparisons of major C, N, and P pools during litter decomposition show the direct contributions of algal biomass to pools at the end of leaf decomposition, as well as indirect effects of algae on other pools, especially those of fungal biomass, remaining litter, and accumulated microbial necromass (**Figure 5**). Algae consistently increased the proportion of initial litter C remaining within litter-periphyton after microbial colonization and decomposition, partly by enhancing accrual of

FIGURE 2 | Mean ± SD weighted effect sizes (log response ratios) of algae on standing litter-periphyton C:N (A,B) or C:P (C,D). Effects are separated into early, mid, or late stages of decomposition (A,C) or averaged throughout the entire decomposition period (B,D). Positive effect sizes indicate algae increase the C:N or C:P of litter-periphyton.

FIGURE 3 | Mean ± SD weighted effect sizes (Hedge's *d*) of algae on N-specific mass loss rates k_N and P-specific mass loss rates k_P during leaf litter decomposition. Positive effect sizes indicate algae increase *k*-values, indicative of faster N or P mineralization in the presence of algae.
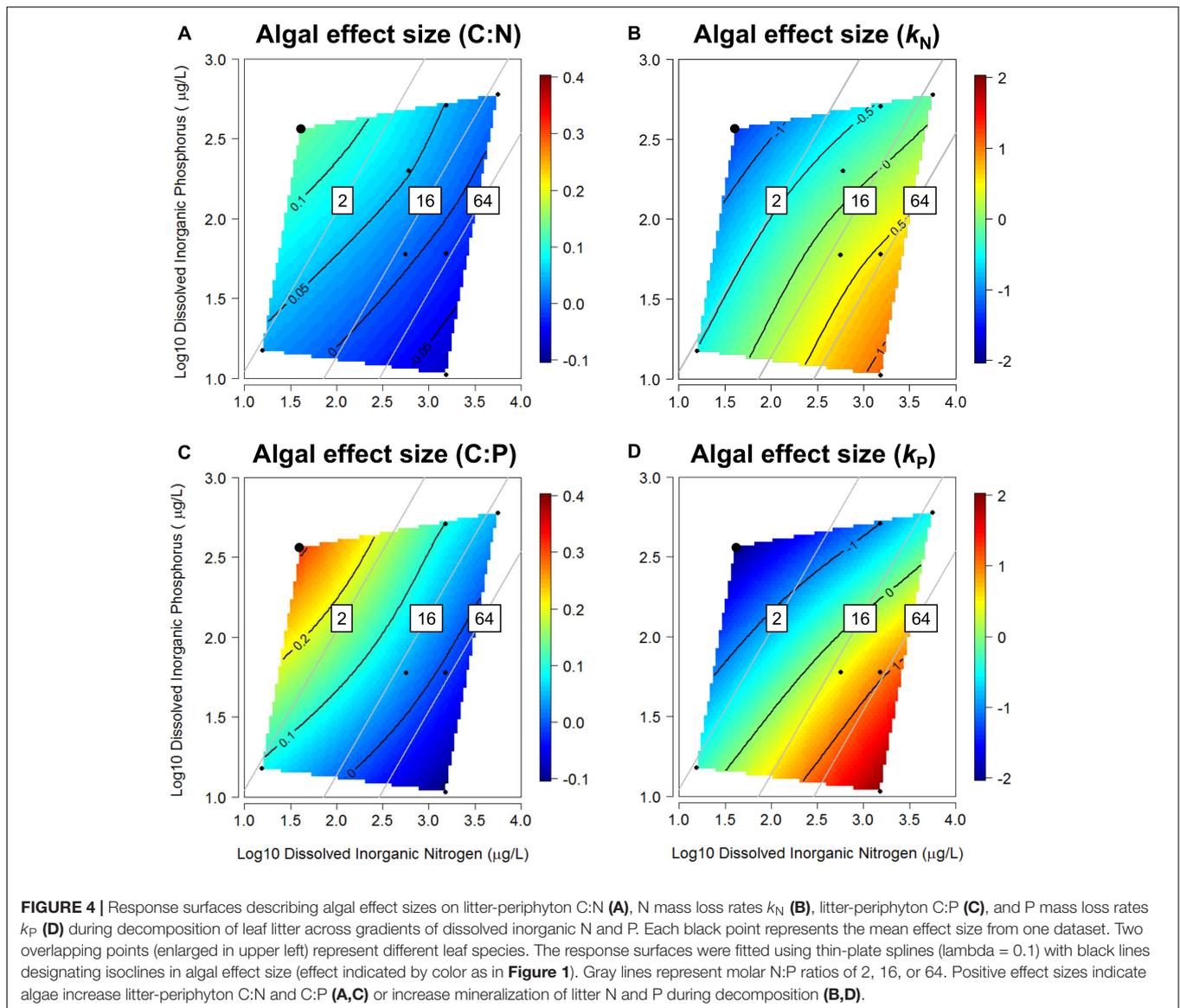
microbial biomass (0.7–10.3% of final total C was algal), but more substantially by increasing C pools remaining, e.g., due to a negative priming effect associated with less degradation of detrital C (**Figure 5A**). Algae similarly contributed 0.9–14.8% of standing litter-periphyton N, approximately equal to fungal N pools in light treatments (5.1–13.1%) and, similar to C pools, algae tended to increase detrital N remaining as litter + microbial necromass at the end of decomposition (**Figure 5B**). Algae also consistently decreased the proportion of N associated with fungi by reducing fungal biomass (**Figure 5B**). Algal effects on P pools were greater, with algae increasing the final litter-periphyton P pools, themselves contributing 2.2–14.9% of litter-periphyton P (**Figure 5C**). The strongest algal effects on litter-periphyton P were by altering the pool of litter + necromass P, likely by both suppressing *P* mass loss and by increasing the accumulation of *P*-rich microbial necromass in these negative priming scenarios (**Figure 5C**). Bacterial pools were consistently a small proportion of litter-periphyton (at most 1.30–4.38% of litter-periphyton P), and did not vary strongly with algal activity.
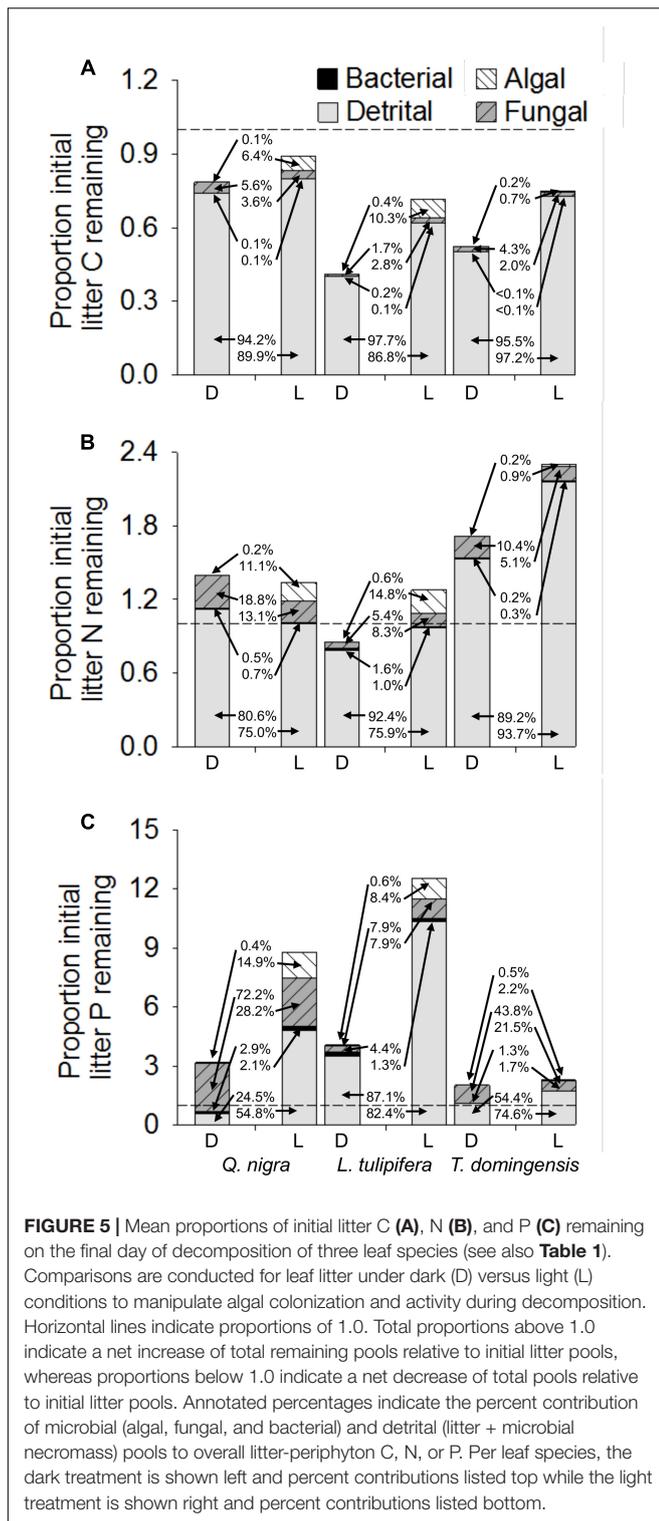
DISCUSSION

Our synthesis shows that algal-mediated priming can affect the stoichiometry of leaf litter decomposition, yet across these studies the effects vary widely in both direction and magnitude. We did not find support for our first hypothesis, as priming intensity and algal-mediated changes in litter stoichiometry did not weaken with increasing dissolved N and P concentrations (Guenet et al., 2010). However, within the bounds of the source datasets (DIN = 15–5600 µg L^{-1} and DIP = 10-600 µg L^{-1}), our synthesis does suggest that dissolved N:P ratios influence priming intensity and algal-mediated shifts in litter-periphyton stoichiometry, especially C:N and k_N. We also did not find support for our second hypothesis, because algae did not consistently alter litter-periphyton C:N or C:P, rather algae increased litter-periphyton C:N and C:P early into decomposition and subsequently decreased C:N and C:P late into decomposition. Moreover, from a subset of studies we found that algae can shift pools of microbial and detrital C, N, and P within decomposing litter-periphyton. As expected from our third hypothesis, we found weak algal effects on N- and P-specific mass loss from litter-periphyton during decomposition, possibly because algal immobilization counterbalances algal effects on heterotrophic mineralization of litter N and P (Halvorson et al., 2016; Elosegi et al., 2018), or perhaps due to the wide variation in priming intensity across datasets. The small sample size and large variation revealed by our meta-analysis suggest that additional studies are needed to further assess the overall priming effect, its dependence on environmental factors such as N:P availability, and its implications for coupled elemental transformations in aquatic ecosystems.

FIGURE 4 | Response surfaces describing algal effect sizes on litter-periphyton C:N **(A)**, N mass loss rates k_N **(B)**, litter-periphyton C:P **(C)**, and P mass loss rates k_P **(D)** during decomposition of leaf litter across gradients of dissolved inorganic N and P. Each black point represents the mean effect size from one dataset. Two overlapping points (enlarged in upper left) represent different leaf species. The response surfaces were fitted using thin-plate splines (lambda = 0.1) with black lines designating isoclines in algal effect size (effect indicated by color as in **Figure 1**). Gray lines represent molar N:P ratios of 2, 16, or 64. Positive effect sizes indicate algae increase litter-periphyton C:N and C:P **(A,C)** or increase mineralization of litter N and P during decomposition **(B,D)**.

Our meta-analysis reveals a striking relationship between algal-mediated priming intensity, shifts in litter-periphyton stoichiometry, and the stoichiometry of dissolved nutrients. Based on greater preferential substrate use of labile algal C at high nutrient concentrations (Guenet et al., 2010), we hypothesized that priming intensity would decline at higher DIN and DIP. However, our survey suggested that, within the ranges of observed N and P concentrations, priming intensity instead varied with dissolved N:P ratios, with positive priming under ostensibly N-replete conditions, and negative priming under ostensibly P-replete conditions. Relatively N-replete conditions (N:P > 64 molar) may induce positive priming because high DIN concentrations stimulate algal growth, but onset of P-limitation may limit algal activity and exudation, providing only a small pool of labile C which can prime microbial heterotrophs, e.g., by supplementing enzyme synthesis (Rier et al., 2007; Ziegler and Lyon, 2010; Danger et al., 2013; Wyatt et al., 2014).

High DIN concentrations further permit greater heterotrophic investment in N-rich enzymes, namely to acquire comparatively limiting litter-associated endogenous P, increasing mineralization of litter C, N, and P and thus increasing litter decomposition via P-mining (**Figure 6A**; Jabiol et al., 2018). In contrast, relatively P-replete conditions (N:P < 16 molar) may induce negative priming because high DIP concentrations, tenably supplemented by algal N-fixation (Smith, 1983), stimulates algal C exudation, which provides a more preferential C substrate for microbial heterotrophs in lieu of the recalcitrant detrital C substrate (Gu and Wyatt, 2016; Halvorson et al., 2016). Moreover, under low dissolved N:P conditions, microbial heterotrophs might compete with algae for a limited pool of DIN, and N supply may be insufficient to support heterotrophic investment in N-costly degradative enzymes, thus limiting degradation of the litter and slowing decomposition (**Figure 6B**; Carreiro et al., 2000; Jabiol et al., 2018). Note that studies rarely reported total dissolved

FIGURE 5 | Mean proportions of initial litter C **(A)**, N **(B)**, and P **(C)** remaining on the final day of decomposition of three leaf species (see also **Table 1**). Comparisons are conducted for leaf litter under dark (D) versus light (L) conditions to manipulate algal colonization and activity during decomposition. Horizontal lines indicate proportions of 1.0. Total proportions above 1.0 indicate a net increase of total remaining pools relative to initial litter pools, whereas proportions below 1.0 indicate a net decrease of total pools relative to initial litter pools. Annotated percentages indicate the percent contribution of microbial (algal, fungal, and bacterial) and detrital (litter + microbial necromass) pools to overall litter-periphyton C, N, or P. Per leaf species, the dark treatment is shown left and percent contributions listed top while the light treatment is shown right and percent contributions listed bottom.

and other environmental conditions, the interactions between N:P availability and priming intensity may partly explain the wide variation of priming effects observed in aquatic ecosystems (Bengtsson et al., 2018).

The roles of algae in litter-periphyton stoichiometry are important for understanding the fate of litter-derived nutrients and food quality for consumers in response to light and nutrient availability across ecosystems (Manning et al., 2015; Warren et al., 2016; Evans-White and Halvorson, 2017). Algae may alter litter-periphyton C:N and C:P directly by introducing pools of exogenous C:N:P through photosynthesis and immobilization, and indirectly by modifying the pool of endogenous litter C:N:P via priming (Danger et al., 2013; Halvorson et al., 2016). Although algae exerted only weak overall effects on litter-periphyton C:N:P throughout decomposition, algal-mediated increases in C:N and C:P early into litter decomposition suggest that algal colonization introduces a high-C:N and C:P pool of initial microbial biomass compared to heterotrophic microbial biomass. At early stages, algae are unlikely to alter litter C:N:P through priming; algal effects mostly likely occur through direct biomass accrual (C fixation), which elevates the pool of litter-periphyton C at the outset of decomposition. Although algae may continue to accrue relatively high-C:N and C:P biomass later into decomposition as well, our study points to a shift during late decomposition, in which algae induce a decrease of litter-periphyton C:N and C:P. This shift is likely driven by two processes: (1) algae can lower the C:N and C:P of litter-periphyton by increasing the total pool of N- and P-rich microbial biomass (including necromass) which lowers litter-periphyton C:N and C:P late into decomposition, relative to litter-periphyton without algae (Manning et al., 2015; Halvorson et al., 2016; see **Figure 5**); and (2) algal indirect effects on endogenous litter C:N:P (elicited via priming) become stronger later into decomposition, with positive priming scenarios decreasing the pool of endogenous litter C and consequently decreasing litter-periphyton C:N and C:P (Huo et al., 2017). Some of these temporal patterns may reflect our method of classifying decomposition stages by % mass loss instead of time, but the former method is preferable to compare litter-periphyton complexes at similar stages of proportional litter degradation and microbial pools accumulated. A method based on time alone would not as readily compare litter of widely differing recalcitrance. Methods quantifying major microbial and litter pools (and fluxes) of C, N, and P could help resolve the observed temporal patterns underlying algal effects on decomposing litter-periphyton C:N:P.

The above temporal trends in litter stoichiometry are reflected in litter-periphyton elemental pools late into decomposition. We were able to assess algal effects on litter-periphyton elemental pools only from negative priming scenarios (**Table 1**). In these scenarios, algae increased total litter-periphyton pools of both C and nutrients compared to algae-absent treatments, reducing the net change in C:N and C:P. Algae also did not consistently increase total N or P in microbial pools, because greater fungal biomass in algal absence replaces the pool of N or P added by algae (**Figure 5**). Algae likely promote increased internal recycling of elements within the litter-periphyton complex by thickening the boundary layer and promoting co-metabolism,
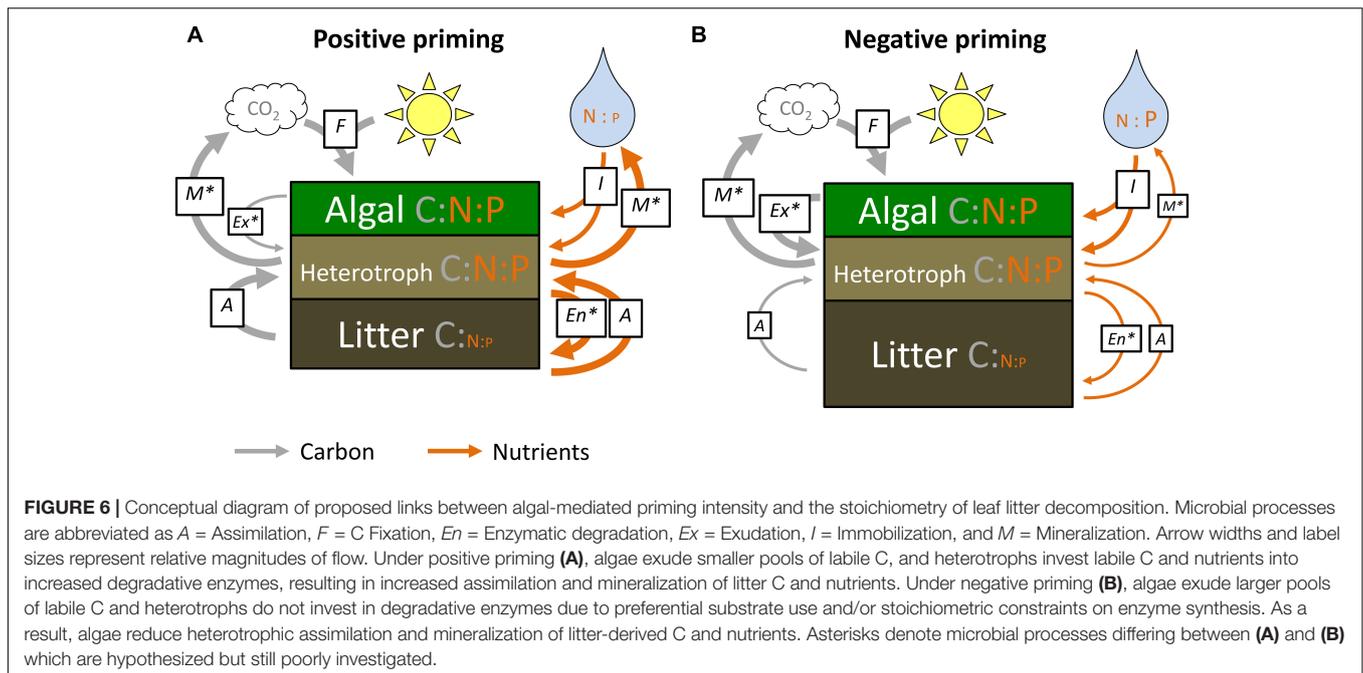
N or P, but these terms would provide a further depiction of the relative availability of each pool of N and P in tandem with algal exudate stoichiometry, because algal exudates may include proteins and other N- or P-containing compounds (Haas and Wild, 2010). Collected across datasets using diverse leaf litter

FIGURE 6 | Conceptual diagram of proposed links between algal-mediated priming intensity and the stoichiometry of leaf litter decomposition. Microbial processes are abbreviated as A = Assimilation, F = C Fixation, En = Enzymatic degradation, Ex = Exudation, I = Immobilization, and M = Mineralization. Arrow widths and label sizes represent relative magnitudes of flow. Under positive priming **(A)**, algae exude smaller pools of labile C, and heterotrophs invest labile C and nutrients into increased degradative enzymes, resulting in increased assimilation and mineralization of litter C and nutrients. Under negative priming **(B)**, algae exude larger pools of labile C and heterotrophs do not invest in degradative enzymes due to preferential substrate use and/or stoichiometric constraints on enzyme synthesis. As a result, algae reduce heterotrophic assimilation and mineralization of litter-derived C and nutrients. Asterisks denote microbial processes differing between **(A)** and **(B)** which are hypothesized but still poorly investigated.

especially in negative priming scenarios (Wetzel, 1993; Halvorson et al., 2016). Though highly variable, algal-mediated shifts in litter-periphyton C:N:P during decomposition could alter the role of leaf litter as a long-term source or sink of dissolved nutrients, potentially affecting ecosystem-level nutrient cycling (Mulholland, 2004; Lin and Webster, 2014).

Algal effects on litter-periphyton C:N:P may partially reflect algal effects on N- and P-specific mass loss from litter-periphyton during decomposition (Soares et al., 2017). Across studies, algae tended to slow N- and P-specific mass loss, likely through a combination of both directly immobilizing exogenous N and P, as well as by indirectly reducing endogenous N and P mineralization by heterotrophs (negative priming; **Figure 6**). Interestingly, the correlation and response surface analyses show algal effects on k_N and k_P reversed from negative at low N:P to positive at higher N:P, suggesting a link with priming intensity. Under positive priming, algae increase N and P mass loss, likely through increased heterotrophic investment in degradative enzymes and mineralization of litter N and P (Rier et al., 2007; Kuzyakov, 2010). Under negative priming, algae reduce N and P mineralization from litter, probably by suppressing heterotrophic investment in enzymes and simultaneously by immobilizing N and P (Blagodatskaya and Kuzyakov, 2008; Halvorson et al., 2019). In this way, algal priming intensity may also strongly affect the fate of endogenous litter N and P, not just litter C. The opposing algal effects on C:N and C:P versus k_N and k_P indicate algal effects on litter-periphyton C loss are relatively stronger than effects on N and P loss. For example, under positive priming scenarios, algae decrease litter-periphyton C:N and C:P despite increasing k_N and k_P, meaning algal-mediated increases in litter C mineralization are stronger than increases in N and P mass loss. At the ecosystem level, our study advances the hypothesis that increased light availability may cause litter-periphyton to serve as

either a stronger sink or a stronger source of dissolved N and P, generally switching from the latter to the former with increasing dissolved N:P ratios. This phenomenon could be relevant for predicting interactions between light and nutrient availability as controls on aquatic ecosystem nutrient dynamics, such as down the river continuum (Fellows et al., 2006; Finlay et al., 2011). Studies tracking coupled elemental flows during decomposition (e.g., using isotopic tracers; Mooshammer et al., 2012; Cheever et al., 2013) would provide a clearer picture of whether these bottom-up shifts are due to altered algal immobilization of N and P, or due to shifts in algal priming of heterotrophic mineralization of litter N and P.

CONCLUSION

Our meta-analysis synthesized existing experiments regarding algal priming intensity and its relationship to ecological stoichiometry during leaf litter decomposition. We found that algae did not consistently alter litter-periphyton C:N:P or N- and P-specific mass loss, but this does not disqualify the ecological significance of algal influence on the stoichiometry of organic matter decomposition. Priming effects are clearly important in some settings, with intensities varying from strongly positive to strongly negative, with clear correlations to N:P availability and links to nutrient mineralization/immobilization (**Table 1** and **Figure 6**; Bengtsson et al., 2018). Moreover, our study represents the first examination of the stoichiometry of algal-mediated priming. Clearly the present meta-analysis would benefit from a larger sample size, given low statistical power (range: 0.05–0.41, **Table 2**), and would also benefit from data generated over a wider array of environmental conditions and investigators. The funnel plots also provide an indicator of small-study effects

or biases, with asymmetry most apparent for algal effects on litter-periphyton C:P (**Supplementary Figure S1B**), suggesting potential inflation of the mean effect size by small datasets. Smaller datasets also appear to exhibit greater absolute effect sizes for k_N and k_P (**Supplementary Figures S1C,D**). Still, the number of datasets is too small to conclude publication bias as a driver of our findings (Jennions et al., 2013), and unlike in some meta-analyses, there may not exist one "true," global priming effect size, given the complexity and variation of interactions revealed by our meta-analysis across different experimental conditions.

Additional tests of algal-mediated priming effects are certainly needed to increase sample sizes and provide a robust assessment of the direction and magnitude of priming effects across a variety of environmental contexts (Bengtsson et al., 2018). Major knowledge gaps revealed by our meta-analysis include (1) determining how overall enzymatic activity and ecoenzymatic stoichiometry relate to the priming effect under different nutrient conditions (Rier et al., 2007; Sinsabaugh and Follstad Shah, 2012; Sinsabaugh et al., 2014), (2) whether priming-induced shifts in net N and P mineralization reflect algal immobilization vs. changes in heterotrophic mineralization of organic N and P, and (3) detailed accounting of C flows between autotrophs (e.g., exudation) and heterotrophs which could explain priming intensity and shifts in C sources contributing to heterotrophic growth or mineralization during organic matter decomposition (**Figure 6**). Our meta-analysis specifically points to a lack of studies measuring processes and fates of elemental currencies beyond C, which is necessary to understand coupled elemental transformations associated with priming. We suggest that experiments would especially benefit from manipulating exogenous and/or endogenous N:P as a potential determinant of priming direction and strength. Such experiments may improve our understanding of N and P availability and stoichiometry as drivers of ecosystem processes (e.g., C storage vs. mineralization) and nutrient feedbacks across ecosystems, especially as N:P shifts with global change (Peñuelas et al., 2013; Kominoski et al., 2015; Guenet et al., 2018).

AUTHOR CONTRIBUTIONS

HH, KK, SF, and RF all conceived and developed the ideas in this manuscript, and aided in the collection of associated unpublished data. HH led the literature survey, meta-analysis, and writing of the manuscript. All authors provided critical feedback during writing.

FUNDING

ACKNOWLEDGMENTS

SUPPLEMENTARY MATERIAL

The Supplementary Material for this article can be found online at: https://www.frontiersin.org/articles/10.3389/feart.2019.00076/full#supplementary-material

REFERENCES

Bärlocher, F. (2005). "Leaf mass loss estimated by litter bag technique," in *Methods to Study Litter Decomposition*, eds M. A. S. Graça, F. Bärlocher, and M. O. Gessner (Dordrecht: Springer), 37–42. doi: 10.1007/1-4020-3466-0_6

Battin, T. J., Besemer, K., Bengtsson, M. M., Romani, A. M., and Packmann, A. I. (2016). The ecology and biogeochemistry of stream biofilms. *Nat. Rev. Microbiol.* 14, 251–263. doi: 10.1038/nrmicro.2016.15

Bengtsson, M. M., Attermeyer, K., and Catalán, N. (2018). Interactive effects on organic matter processing from soils to the ocean: are priming effects relevant in aquatic ecosystems? *Hydrobiologia* 822, 1–17. doi: 10.1007/s10750-018-3672-2

Bianchi, T. S., Thornton, D. C. O., Yvon-Lewis, S. A., King, G. M., Eglinton, T. I., Shields, M. R., et al. (2015). Positive priming of terrestrially derived dissolved organic matter in a freshwater microcosm system. *Geophys. Res. Lett.* 42, 5460–5467. doi: 10.1002/2015GL064765

Blagodatskaya, E., and Kuzyakov, Y. (2008). Mechanisms of real and apparent priming effects on their dependence on soil microbial biomass and community structure: critical review. *Biol. Fert. Soils* 45, 115–131. doi: 10.1007/s00374-008-0334-y

Carreiro, M. M., Sinsabaugh, R. L., Repert, D. A., and Parkhurst, D. F. (2000). Microbial enzyme shifts explain litter decay responses to simulated nitrogen deposition. *Ecology* 81, 2359–2365. doi: 10.1890/0012-9658(2000)081[2359:MESELD]2.0.CO;2

Catalán, N., Kellerman, A. M., Peter, H., Carmona, F., and Tranvik, L. J. (2015). Absence of a priming effect on dissolved organic carbon degradation in lake water. *Limnol. Oceanogr.* 60, 159–168. doi: 10.1002/lno.10016

Cebrian, J. (1999). Patterns in the fate of production in plant communities. *Am. Nat.* 154, 449–468. doi: 10.1086/303244

Champely, S. (2018). *Package 'pwr': Basic Functions for Power Analsis. R Package Version 1.2-2.* Available at: https://cran.r-project.org/web/packages/pwr/pwr.pdf (accessed March 03, 2018).

Cheever, B. M., Webster, J. R., Bilger, E. E., and Thomas, S. A. (2013). The relative importance of exogenous and substrate derived nitrogen for microbial growth during leaf decomposition. *Ecology* 94, 1614–1625. doi: 10.1890/12-1339.1

Chen, R., Senbayram, M., Blagodatsky, S., Myachina, O., Dittert, K., Lin, X., et al. (2014). Soil C and N availability determine the priming effect: microbial N mining and stoichiometric decomposition theories. *Glob. Chang. Biol.* 20, 2356–2367. doi: 10.1111/gcb.12475

Cheng, W., Parton, W. J., Gonzalez-Meler, M. A., Phillips, R., Asao, S., McNickle, G. G., et al. (2014) Synthesis and modeling perspectives of rhizosphere priming. *New Phytol.* 201, 31–44. doi: 10.1111/nph.12440

Danger, M., Cornut, J., Chauvet, E., Chavez, P., Elger, A., and Lecerf, A. (2013). Benthic algae stimulate leaf litter decomposition in detritus-based headwater streams: a case of aquatic priming effect? *Ecology* 94, 1604–1613. doi: 10.1890/12-0606.1

Demars, B., Friberg, N., Kemp, J. L., and Thornton, B. (2018). Reciprocal carbon subsidies between autotrophs and bacteria in stream food webs under stoichiometric constraints. *bioRXiv* [Preprint]. doi: 10.1101/447987

Elosegi, A., Nicolás, A., and Richardson, J. S. (2018). Priming of leaf litter decomposition by algae seems of minor importance in natural streams during autumn. *PLoS One* 13:e0200180. doi: 10.1371/journal.pone.0200180

Evans-White, M. A., and Halvorson, H. M. (2017). Comparing the ecological stoichiometry in green and brown food webs - A review and meta-analysis of freshwater food webs. *Front. Microbiol.* 8:1184. doi: 10.3389/fmicb.2017.01184

Fang, Y., Nazaries, L., Singh, B. K., and Singh, B. P. (2018). Microbial mechanisms of carbon priming effects revealed during the interaction of crop residue and nutrient inputs in contrasting soils. *Glob. Chang. Biol.* 24, 2775–2790. doi: 10.1111/gcb.14154

Fellows, C. S., Valett, H. M., Dahm, C. N., Mulholland, P. J., and Thomas, S. A. (2006). Coupling nutrient uptake and energy flow in headwater streams. *Ecosystems* 9, 788–804. doi: 10.1007/s10021-006-0005-5

Finlay, J. C., Hood, J. M., Limm, M. P., Power, M. E., Schade, J. D., and Welter, J. R. (2011). Light-mediated thresholds in stream-water nutrient composition in a river network. *Ecology* 92, 140–150. doi: 10.1890/09-2243.1

Godwin, C. M., and Cotner, J. B. (2015). Aquatic heterotrophic bacteria have highly flexible phosphorus content and biomass stoichiometry. *ISME J.* 9, 2324–2327. doi: 10.1038/ismej.2015.34

Greenwood, J. L., and Rosemond, A. D. (2005). Periphyton response to long-term nutrient enrichment in a shaded headwater stream. *Can. J. Fish. Aquat. Sci.* 62, 2033–2045. doi: 10.1139/f05-117

Gu, L. Y., and Wyatt, K. H. (2016). Light availability regulates the response of algae and heterotrophic bacteria to elevated nutrient levels and warming in a northern boreal peatland. *Freshw. Biol.* 61, 1442–1453. doi: 10.1111/fwb.12783

Guenet, B., Camino-Serrano, M., Ciais, P., Tifafi, M., Maignan, F., Soong, J. L., et al. (2018). Impact of priming on global soil carbon stocks. *Glob. Chang. Biol.* 24, 1873–1883. doi: 10.1111/gcb.14069

Guenet, B., Danger, M., Abbadie, L., and Lacroix, G. (2010). Priming effect: bridging the gap between terrestrial and aquatic ecology. *Ecology* 91, 2850–2861. doi: 10.1890/09-1968.1

Guillemette, F., Leigh McCallister, S., and del Giorgio, P. A. (2016). Selective consumption and metabolic allocation of terrestrial and algal carbon determine allochthony in lake bacteria. *ISME J.* 10, 1373–1382. doi: 10.1038/ismej.2015.215

Gulis, V., Kuehn, K. A., Schoettle, L. N., Leach, D., Benstead, J. P., and Rosemond, A. D. (2017). Changes in nutrient stoichiometry, elemental homeostasis and growth rate of aquatic litter-associated fungi in response to inorganic nutrient supply. *ISME J.* 11, 2729–2739. doi: 10.1038/ismej.2017.123

Haas, A. F., and Wild, C. (2010). Composition analysis of organic matter released by cosmopolitan coral reef-associated green algae. *Aquat. Biol.* 10, 131–138. doi: 10.3354/ab00271

Halvorson, H. M., Barry, J. R., Lodato, M. B., Findlay, R. H., Francoeur, S. N., and Kuehn, K. A. (2019). Periphytic algae decouple fungal activity from leaf litter decomposition via negative priming. *Funct. Ecol.* 33, 188–201. doi: 10.1111/1365-2435.13235

Halvorson, H. M., Scott, E. E., Entrekin, S. A., Evans-White, M. A., and Scott, J. T. (2016). Light and dissolved phosphorus interactively affect microbial metabolism, stoichiometry and decomposition of leaf litter. *Freshw. Biol.* 61, 1006–1019. doi: 10.1111/fwb.12763

Hedges, L. V., and Olkin, I. (1985). *Statistical Methods for Meta-Analysis*. Orlando, FL: Academic Press.

Hotchkiss, E. R., Hall, R. O., Baker, M. A., Rosi-Marshall, E. J., and Tank, J. L. (2014). Modeling priming effects on microbial consumption of dissolved organic carbon in rivers. *J. Geophys. Res. Biogeosci.* 119, 982–995. doi: 10.1002/2013JG002599

Huo, C., Luo, Y., and Cheng, W. (2017). Rhizosphere priming effect: a meta-analysis. *Soil Biol. Biochem.* 111, 78–84. doi: 10.1016/j.soilbio.2017.04.003

Jabiol, J., Cornut, J., Tlili, A., and Gessner, M. O. (2018). Interactive effects of dissolved nitrogen, phosphorus and litter chemistry on stream fungal decomposers. *FEMS Microbiol. Ecol.* 94:fiy151. doi: 10.1093/femsec/fiy151

Jennions, M. D., Lortie, C. J., Rosenberg, M. S., and Rothstein, H. R. (2013). "Publication and related biases," in *Handbook of Meta-Analysis in Ecology and Evolution*, eds J. Koricheva, J. Gurvetich, and K. Mengersen (Princeton, NJ: Princeton University Press), 207–236.

Kahlert, M. (1998). C:N:P ratios of freshwater benthic algae. *Arch. Hydrobiol.* 51, 105–114. doi: 10.1111/gcb.13205

Kominoski, J. S., Rosemond, A. D., Benstead, J. P., Gulis, V., Maerz, J., and Manning, D. W. P. (2015). Low-to-moderate nitrogen and phosphorus concentrations accelerate microbially driven litter breakdown rates. *Ecol. Appl.* 25, 856–865. doi: 10.1890/14-1113.1.sm

Kuehn, K. A., Francoeur, S. N., Findlay, R. H., and Neely, R. K. (2014). Priming in the microbial landscape: periphytic algal stimulation of litter-associated microbial decomposers. *Ecology* 95, 749–762. doi: 10.1890/13-0430.1

Kuzyakov, Y. (2010). Priming effects: interactions between living and dead organic matter. *Soil Biol. Biochem.* 42, 1363–1371. doi: 10.1016/J.SOILBIO.2010.04.003

Li, L.-J., Zhu-Barker, X., Ye, R., Doane, T. A., and Horwath, W. R. (2018). Soil microbial biomass size and soil carbon influence the priming effect from carbon inputs depending on nitrogen availability. *Soil Biol. Biochem.* 119, 41–49. doi: 10.1016/J.SOILBIO.2018.01.003

Lin, L., and Webster, J. R. (2014). Detritus decomposition and nutrient dynamics in a forested headwater stream. *Ecol. Model.* 293, 58–68. doi: 10.1016/j.ecolmodel.2013.12.013

Manning, D. W. P., Rosemond, A. D., Kominoski, J. S., Gulis, V., Benstead, J. P., and Maerz, J. C. (2015). Detrital stoichiometry as a critical nexus for the effects of streamwater nutrients on leaf litter breakdown rates. *Ecology* 96, 2214–2224. doi: 10.1890/14-1582.1

Manzoni, S., Trofymow, J. A., Jackson, R. B., and Porporato, A. (2010). Stoichiometric controls on carbon, nitrogen, and phosphorus dynamics in decomposing litter. *Ecol. Monogr.* 80, 89–106. doi: 10.1890/09-0179.1

Meier, I. C., Finzi, A. C., and Phillips, R. P. (2017). Root exudates increase N availability by stimulating microbial turnover of fast-cycling N pools. *Soil Biol. Biochem.* 106, 119–128. doi: 10.1016/J.SOILBIO.2016.12.004

Moore, J. C., Berlow, E. L., Coleman, D. C., Ruiter, P. C., Dong, Q., Hastings, A., et al. (2004). Detritus, trophic dynamics and biodiversity. *Ecol. Lett.* 7, 584–600. doi: 10.1111/j.1461-0248.2004.00606.x

Moorhead, D. L., and Sinsabaugh, R. L. (2006). A theoretical model of litter decay and microbial interaction. *Ecol. Monogr.* 76, 151–174. doi: 10.1890/0012-9615(2006)076[0151:ATMOLD]2.0.CO;2

Mooshammer, M., Wanek, W., Schnecker, J., Wild, B., Leitner, S., Hofhansl, F., et al. (2012). Stoichiometric controls of nitrogen and phosphorus cycling in decomposing beech leaf litter. *Ecology* 93, 770–782. doi: 10.1890/11-0721.1

Mulholland, P. J. (2004). The importance of in-stream uptake for regulating stream concentrations and outputs of N and P from a forested watershed: evidence from long-term chemistry records for Walker Branch Watershed. *Biogeochemistry* 70, 403–426. doi: 10.1007/s10533-004-0364-y

Nychka, D., Furrer, R., Paige, J., and Sain, S. (2018). *Package 'fields': Tools for Spatial Data. R Package Version 9.6*. Available at: https://cran.r-project.org/web/packages/fields/fields.pdf [accessed January 15, 2018].

Pasek, J. (2018). *Package Weights: Weighting and Weighted Statistics. R Package Version 1.0*. Available at: https://cran.r-project.org/web/packages/weights/weights.pdf [accessed October 16, 2018].

Peñuelas, J., Poulter, B., Sardans, J., Ciais, P., van der Velde, M., Bopp, L., et al. (2013). Human-induced nitrogen-phosphorus imbalances alter natural and managed ecosystems across the globe. *Nat. Commun.* 4:2934. doi: 10.1038/ncomms3934

R Core Team (2018). *R: A Language and Environmental for Statistical Computing*. Vienna: R Foundation for Statistical Computing.

Rier, S. T., Kuehn, K. A., and Francoeur, S. N. (2007). Algal regulation of extracellular enzyme activity in stream microbial communities associated with inert substrata and detritus. *J. North Am. Benthol. Soc.* 26, 439–449. doi: 10.1899/06-080.1

Romaní, A. M., Fischer, H., Mille-Lindblom, C., and Tranvik, L. J. (2006). Interactions of bacteria and fungi on decomposing litter: differential extracellular enzyme activities. *Ecology* 87, 2559–2569. doi: 10.1890/0012-9658(2006)87[2559:IOBAFO]2.0.CO;2

Rosenberg, M. S. (2013). "Moment and least-squares based approaches to meta-analytic inference," in *Handbook of Meta-Analysis in Ecology and Evolution*, eds J. Koricheva, J. Gurvetich, and K. Mengersen (Princeton, NJ: Princeton University Press), 108–124.

Rosenberg, M. S., Rothstein, H. R., and Gurevitch, J. (2013). "Effect sizes: conventional choices and calculations," in *Handbook of Meta-Analysis in*

Ecology and Evolution, eds J. Koricheva, J. Gurvetich, and K. Mengersen (Princeton, NJ: Princeton University Press), 61–71.

Scott, J. T., Back, J. A., Taylor, J. M., and King, R. S. (2008). Does nutrient enrichment decouple algal–bacterial production in periphyton? *J. North Am. Benthol. Soc.* 27, 332–344. doi: 10.1899/07-108.1

Senior, A. M., Grueber, C. E., Kamiya, T., Lagisz, M., O'Dwyer, K., Santos, E. S. A., et al. (2016). Heterogeneity in ecological and evolutionary meta-analyses: its magnitude and implications. *Ecology* 97, 3293–3299. doi: 10.1002/ecy.1591

Sinsabaugh, R. L., Belnap, J., Findlay, S. G., Follstad Shah, J. J., Hill, B. H., Kuehn, K. A., et al. (2014). Extracellular enzyme kinetics scale with resource availability. *Biogeochemistry* 121, 287–304. doi: 10.1007/s10533-014-0030-y

Sinsabaugh, R. L., and Follstad Shah, J. J. (2012). Ecoenzymatic stoichiometry and ecological theory. *Annu. Rev. Ecol. Evol. Syst.* 43, 313–343. doi: 10.1146/annurev-ecolsys-071112-124414

Smith, V. H. (1983). Low nitrogen to phosphorus ratios favor dominance by blue-green algae in lake phytoplankton. *Science* 221, 669–671. doi: 10.1126/science.221.4611.669

Soares, M., Kritzberg, E. S., and Rousk, J. (2017). Labile carbon "primes" fungal use of nitrogen from submerged leaf litter. *FEMS Microbiol. Ecol.* 93, fix110. doi: 10.1093/femsec/fix110

Sperfeld, E., Raubenheimer, D., and Wacker, A. (2016). Bridging factorial and gradient concepts of resource co-limitation: towards a general framework applied to consumers. *Ecol. Lett.* 19, 201–215. doi: 10.1111/ele.12554

Sterne, J. A. C., and Harbord, R. M. (2004). Funnel plots in meta-analysis. *Stata J.* 4, 127–141. doi: 10.1177/1536867X0400400204

Sterner, R. W., and Elser, J. J. (2002). *Ecological Stoichiometry: The Biology of Elements from Molecules to the Biosphere*. Princeton, NJ: Princeton University Press.

Wagner, K., Bengtsson, M. M., Findlay, R. H., Battin, T. J., and Ulseth, A. J. (2017). High light intensity mediates a shift from allochthonous to autochthonous carbon use in phototrophic stream biofilms. *J. Geophys. Res. Biogeosci.* 122, 1806–1820. doi: 10.1002/2016JG003727

Warren, D. R., Keeton, W. S., Kiffney, P. M., Kaylor, M. J., Bechtold, H. A., and Magee, J. (2016). Changing forests-changing streams: riparian forest stand development and ecosystem function in temperate headwaters. *Ecosphere* 7:e01435. doi: 10.1002/ecs2.1435

Wetzel, R. G. (1993). Microcommunities and microgradients: linking nutrient regeneration, microbial mutualism, and high sustained aquatic primary production. *Aquat. Ecol.* 27, 3–9. doi: 10.1007/BF02336924

Wyatt, K. H., Tellez, E., Woodke, R. L., Bidner, R. J., and Davis, I. R. (2014). Effects of nutrient limitation on the release and use of dissolved organic carbon from benthic algae in Lake Michigan. *Freshw. Sci.* 33, 557–567. doi: 10.1086/675453

Ziegler, S. A., and Lyon, D. R. (2010). Factors regulating epilithic biofilm carbon cycling and release with nutrient enrichment in headwater streams. *Hydrobiologia* 657, 71–88. doi: 10.1007/s10750-010-0296-6